PAPER

Check for updates

Reverse sequence polymerization-induced self-assembly in aqueous media: a counter-intuitive approach to sterically-stabilized diblock copolymer nano-objects†

Nicholas J. W. Penfold, [ID] [a] Thomas J. Neal, [ID] *[a] Corentin Plait,[a] Andrew E. Leigh,[a] Gwen Chimonides,[a] Mark J. Smallridge[b] and Steven P. Armes [ID] *[a]

Polymerization-induced self-assembly (PISA) is a powerful platform technology for the efficient synthesis of block copolymer nanoparticles in many types of solvents, including water. In PISA, a soluble precursor block is used to grow a second insoluble block, which leads to *in situ* self-assembly of the block copolymer chains. Thus, in the case of aqueous PISA, the water-soluble block is always prepared first because this confers steric stabilization. Herein, we challenge this paradigm by demonstrating that amphiphilic diblock copolymer chains can be prepared in water by preparing the hydrophobic block first *via* reversible addition–fragmentation chain transfer (RAFT) polymerization. This counter-intuitive *reverse sequence* PISA formulation utilizes an ionic RAFT agent to conduct the RAFT aqueous dispersion polymerization of 2-hydroxypropyl methacrylate (HPMA), which results in the formation of charge-stabilized PHPMA latex particles of ∼500 nm diameter. Initial attempts to chain-extend these hydrophobic PHPMA chains with water-miscible monomers such as glycerol monomethacrylate (GMA) were unsuccessful, with only uncontrolled free radical polymerization being observed in the aqueous phase. However, using a water-immiscible monomer such as isopropylideneglycerol methacrylate (IPGMA) enabled the synthesis of charge-stabilized PHPMA-PIPGMA latex particles. Subsequent acid hydrolysis of the PIPGMA block led to the *in situ* formation of sterically-stabilized PHPMA-PGMA diblock copolymer spheres. Alternatively, dissolution of the precursor PHPMA latex in a methanol/water binary mixture enables RAFT solution polymerization of water-miscible monomers such as GMA or *N,N'*-dimethylacrylamide (DMAC) to be achieved with good control. The resulting amphiphilic diblock copolymer chains then undergo self-assembly in aqueous solution after removal of the methanol co-solvent. Finally, this *reverse sequence* PISA protocol can also be applied to other vinyl monomers such as 2-methoxyethyl methacrylate (MOEMA) or diacetone acrylamide (DAAM), which significantly broadens its scope.

[a]*Dainton Building, Department of Chemistry, The University of Sheffield, Brook Hill, Sheffield, South Yorkshire, S3 7HF, UK. E-mail: s.p.armes@sheffield.ac.uk, tneal@ed.ac.uk*
[b]*GEO Specialty Chemicals, Hythe, Southampton, Hampshire SO45 3ZG, UK*
†Electronic supplementary information (ESI) available. See DOI: https://doi.org/10.1039/d2py01064j

Introduction

Over the past decade it has become clear that polymerization-induced self-assembly (PISA) is a powerful and versatile platform technology for the convenient synthesis of a wide range of block copolymer nano-objects in the form of concentrated colloidal dispersions.[1–11] Typically, PISA involves growing a polymer chain from one end of a precursor chain using an appropriate monomer in a suitable solvent. The second chain becomes insoluble when it reaches a certain critical mean degree of polymerization: this induces micellar nucleation and leads to the formation of sterically-stabilized diblock copolymer nanoparticles.[12–15] Many vinyl monomers have been used to prepare such nanoparticles and most of these studies have employed reversible addition–fragmentation chain transfer (RAFT) polymerization.[16–19] This is no doubt because this technique is highly tolerant of monomer functionality.[19,20]

It is well-established that PISA can be conducted in many different types of solvents.[21–31] In the case of water, PISA can be performed using either water-miscible or water-immiscible monomers *via* either aqueous dispersion polymerization or aqueous emulsion polymerization, respectively.[32–67] For such aqueous PISA formulations, it is seemingly essential that the hydrophilic block must be prepared first to ensure that colloidal stability is retained *via* a steric stabilization mechanism.

Recently, we have challenged this paradigm by demonstrating that the *hydrophobic* water-insoluble block can be prepared before generating the hydrophilic block: this new approach is termed *reverse sequence* PISA.[68] Herein, we report on our new experiments based on this counter-intuitive strategy. More specifically, we conduct the RAFT aqueous dispersion of 2-hydroxypropyl methacrylate (HPMA) and the RAFT aqueous emulsion polymerization of 2-methoxyethyl methacrylate (MOEMA)[15] using a previously reported cationic morpholine-functional RAFT agent known as MPETTC (Scheme 1).[69] At low pH, the morpholine end-groups become protonated, which leads to the formation of a cationic precursor latex that remains colloidally stable *via* a charge stabilization mechanism. Two methods were subsequently explored to chain-extend the latex and hence introduce an appropriate steric stabilizer block. The first method involved dissolution of the hydrophobic precursor latex with a suitable water-miscible co-solvent, with subsequent polymerization of a hydrophilic monomer to produce the steric stabilizer block *via* RAFT solution polymerization. The second method involved extending the hydrophobic chains *via* RAFT seeded emulsion polymerization using a second water-immiscible monomer, isopropylideneglycerol monomethacrylate (IPGMA). Again, the resulting diblock copolymer latex remains colloidally stable owing to charge stabilization. Subsequently, the acetone protecting groups on the PIPGMA chains can be removed *via* acid hydrolysis to generate an amphiphilic PHPMA-PGMA diblock copolymer that self-assembles *in situ* to form sterically-stabilized diblock copolymer nano-objects. In addition, the RAFT aqueous dispersion polymerization of diacetone acrylamide (DAAM) using a carboxylic acid-based RAFT agent at pH 7 is briefly explored.

Results and discussion

Synthesis of latex precursors *via* RAFT aqueous dispersion polymerization

Kinetic data were obtained for the RAFT aqueous dispersion polymerization of HPMA at 56 °C by periodic sampling of the reaction mixture followed by ^{1}H NMR spectroscopy studies and DMF GPC analysis. This scoping experiment was performed at pH 3 by targeting a mean degree of polymerization (DP) of 140 for the PHPMA chains at 10% w/w solids. The conversion *vs.* time curve and corresponding semi-logarithmic plot are

shown in Fig. S1.† Initially, a relatively slow RAFT solution polymerization was observed, with only 43% conversion being achieved after 1.5 h at 56 °C. Thereafter, a gradual increase in turbidity indicated micellar nucleation; this coincides with a dramatic increase in the rate of polymerization, with more than 99% conversion being obtained within 3 h. Similar observations have been reported for conventional aqueous PISA syntheses.[70–72] Visual inspection of the final latex dispersion indicated a milky-white, free-flowing fluid (see Fig. 1A).

Importantly, the evolution in M_n is linear with monomer conversion and the relatively narrow molecular weight distributions ($M_w/M_n < 1.15$) confirm that this polymerization proceeds with good RAFT control.[73–77] Scanning electron


Fig. 1 (a) SEM image recorded for a dried PHPMA$_{140}$ latex, indicating its spherical morphology (digital photograph of a 10% w/w aqueous dispersion; see inset). (b) Intensity-average particle size distribution obtained by dynamic light scattering analysis of a 0.1% w/w PHPMA$_{140}$ latex at pH 3. (c) Variation in DLS diameter and zeta potential with pH for this charge-stabilized PHPMA$_{140}$ latex [a 0.1% w/w aqueous dispersion in 1 mM KCl was initially prepared at pH 3 and the solution pH was adjusted using KOH or HCl].

Scheme 1 Schematic cartoon of the RAFT aqueous dispersion polymerization of HPMA using a cationic morpholine-functionalized RAFT agent (MPETTC) and an azo initiator (AIBA) at pH 3 to yield a charge-stabilized precursor PHPMA latex at 56 °C.

microscopy (SEM) images revealed a polydisperse spherical morphology with a number-average SEM diameter of 432 ± 78 nm (see Fig. 1a). This is consistent with dynamic light scattering (DLS) studies, which indicate a z-average diameter of 512 ± 172 nm (see Fig. 1b). Such latex particles are much larger than those usually obtained for conventional aqueous PISA syntheses of sterically-stabilized diblock copolymer nanoparticles, for which mean diameters of less than 100 nm are typically obtained when targeting spheres.[56,60,78,79] In the present study, the weakly hydrophobic nature of the PHPMA chains results in their partial plasticization by water[80–82] and hence a somewhat larger than expected latex diameter. Indeed, higher magnification SEM images suggest that some degree of dehydration of the PHPMA latex particle occurs under the ultrahigh vacuum conditions required for this technique (see Fig. S2†). It is well-known that ionic RAFT end-groups can have a dramatic effect on the electrophoretic footprint[39,50,69,83,84] and colloidal stability[85] of block copolymer nano-objects. Accordingly, the pH-responsive behavior of this PHPMA$_{140}$ latex was examined using DLS and aqueous electrophoresis (see Fig. 1C). Zeta potentials of approximately +40 to +50 mV were observed between pH 2.5 and pH 4.5 owing to protonation of the morpholine-based RAFT groups located at the latex surface. Above pH 4.5, these tertiary amine groups gradually become deprotonated, leading to an isoelectric point at around pH 7. Below pH 2.5, the excess acid acts as a salt and screens the cationic surface charge, leading to lower zeta potentials. DLS studies indicate a colloid stability window from pH 1.8 to pH 5.6; the latex particles retain a sufficiently high zeta potential over this pH range to remain stable with respect to aggregation.

Next, the target PHPMA DP was systematically varied from 60 to 200 (see Table S1†). High HPMA conversions (>99%) were achieved in all cases and relatively narrow, unimodal molecular weight distributions (see Fig. 2a) were indicated by DMF GPC analysis. Furthermore, the linear relationship between M_n and the target PHPMA DP (combined with dispersities of less than 1.13) indicate that good RAFT control was achieved for such surfactant-free aqueous PISA syntheses (see Fig. 2b). Each of these eight latexes was diluted to 0.1% w/w (using 1 mM KCl adjusted to pH 3) to afford dispersions for DLS and aqueous electrophoresis studies (see Fig. 2C). Unexpectedly, the latex with the lowest target DP (PHPMA$_{60}$) proved to be unstable with respect to dilution and became solubilized, as judged by its relatively low scattered light intensity. However, with the benefit of hindsight this is perhaps not surprising: it is well known that similarly short PHPMA blocks can become water-dispersible when conjugated to hydrophilic blocks.[81] In contrast, each of the other seven PHPMA latexes proved to be stable to dilution. Zeta potentials of approximately +50 mV were determined for this latex series regardless of the target PHPMA DP (see Fig. 2C). Similarly, there was surprisingly little change in z-average diameter when varying the PHPMA DP from 80 to 160. These observations suggest that at least some (perhaps most) of the cationic morpholine RAFT end-groups remain buried within the interior of the latex par-
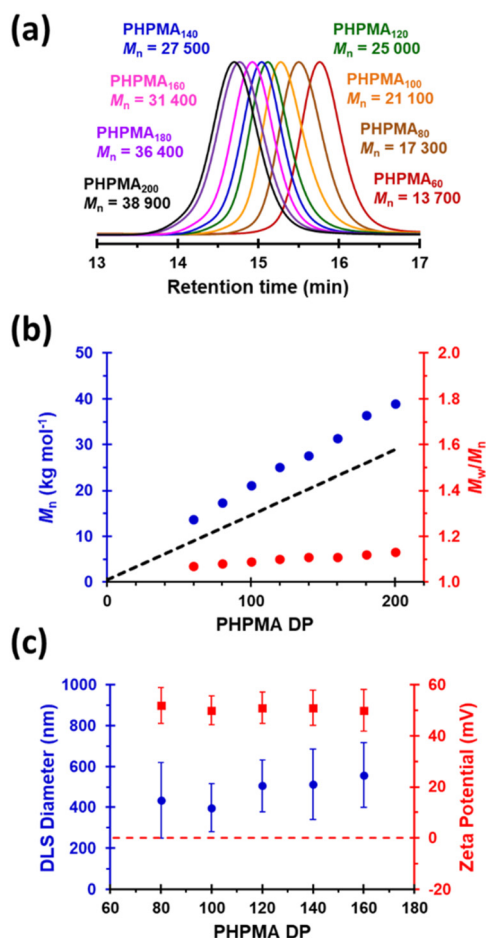
Fig. 2 (a) Normalized DMF GPC curves (refractive index detector; calibrated against a series of poly(methyl methacrylate) standards) recorded for eight PHPMA latexes prepared using MPETTC RAFT agent where the PHPMA DP was systematically varied from 60 to 200. (b) Linear evolution in number-average molecular weight (M_n) and dispersity (M_w/M_n) with increasing target PHPMA DP for the same series of eight PHPMA latexes (the dashed line indicates the theoretical M_n). (c) Variation in z-average diameter and zeta potential with target PHPMA DP for the same series of eight PHPMA latexes.

ticles, rather than being exclusively located at their surface. DLS studies also indicated that PHPMA latexes with DPs greater than 160 were relatively polydisperse and contained some macroscopic precipitate. This suggests that a DP of 160 may represent a realistic upper limit for such aqueous PISA syntheses, at least under the stated conditions. Nevertheless, in principle this should be sufficient to access sphere and worm morphologies via subsequent chain extension experiments using appropriate water-soluble methacrylic monomers.[86,87] Many RAFT agents contain a carboxylic acid group.[88,89] In part, this is because such functionality usually ensures that these compounds exist as solids at ambient temperature, which reduces their malodor. In the context of the present study, we wanted to examine whether carboxylic acid-based RAFT agents might offer the opportunity to conduct the

surfactant-free RAFT aqueous dispersion polymerization of HPMA at pH 7, *i.e.* under conditions where ionization should confer negative surface charge *via* anionic carboxylate groups. Accordingly, we attempted the synthesis of PHPMA₉₀ latexes using a carboxylic acid-functionalized trithiocarbonate-based RAFT agent known as PETTC (see Scheme S1† and Experimental section for further details).[90,91] Indeed, these syntheses yielded free-flowing, milky-white dispersions. ^{1}H NMR spectroscopy and DMF GPC analysis indicated high conversion (>99%) with the HPMA polymerization proceeding under RAFT control (M_n = 22 400, M_w/M_n = 1.12). Furthermore, SEM and DLS studies indicated polydisperse, anionic spherical latexes with a zeta potential of -52 ± 7 mV (see Fig. S3†). Interestingly, such latexes were somewhat smaller (z-average diameter = 213 ± 29 nm) than the corresponding cationic latexes. We hypothesize that conducting these experiments at higher temperatures (70 °C *vs.* 56 °C) resulted in somewhat less hydrated PHPMA latexes and therefore smaller particles. In the remainder of this manuscript, we focus mainly on chain extension experiments conducted using cationic PHPMA latexes prepared using MPETTC. We have chosen to include the synthesis and characterization details for the anionic PHPMA latexes prepared using PETTC because such precursor particles exhibit complementary pH-sensitive behavior and hence may be of interest for specific applications.

Synthesis of PHPMA-PGMA diblock copolymer nanoparticles

Next, chain extension of the cationic PHPMA₁₄₀ precursor was attempted in aqueous media using glycerol monomethacrylate (GMA) targeting PHPMA₁₄₀-PGMA₅₆ diblock copolymer nano-objects. In an initial scoping experiment, GMA monomer was simply added to the as-synthesized aqueous PHPMA₁₄₀ latex (prepared using MPETTC) and allowed to polymerize for 16 h at 56 °C without any additional AIBA initiator. Unfortunately, DMF GPC analysis (using refractive index and UV detectors in tandem) indicated that only uncontrolled free radical solution polymerization of the GMA had occurred, with the production of water-soluble PGMA homopolymer chains rather than the desired diblock copolymer nano-objects (see Fig. S4†). With the benefit of hindsight, this is because the aqueous phase contained unreacted initiator and there is no physical reason for the water-miscible GMA monomer to enter the PHPMA latex particles (which contain the buried RAFT chain-ends). In view of these negative results, the PHPMA latex synthesis was repeated in the absence of any azo initiator using a blue LED source (λ_{max} = 395 nm, 0.37 mW cm⁻²).[92–97] This photoinitiated RAFT protocol[97–100] (see ESI; pages S15 and S16†) afforded colloidally stable PHPMA₁₄₅ latex particles at 10% solids (>99% conversion) and DMF GPC analysis indicated good RAFT control (M_n = 26 900; M_w/M_n = 1.10). However, subsequent photoinitiation of GMA in the presence of this PHPMA latex again led to the formation of a substantial fraction of polydisperse water-soluble PGMA chains that contained no RAFT chain-ends (see Fig. S5†). Presumably, this is because photoinitiation generates *water-soluble* radicals, which

then polymerize the GMA monomer in the aqueous continuous phase *via* uncontrolled free radical polymerization, rather than within the latex particles.

To circumvent this problem, we added sufficient methanol (32% v/v) to the aqueous precursor latex to form soluble PHPMA chains, which enables their efficient chain extension to be achieved *via* RAFT solution polymerization of GMA in an aqueous methanol milieu in the absence of any additional AIBA initiator. In such syntheses, GMA conversions of 98–99% were routinely obtained. Moreover, DMF GPC analysis indicated efficient chain extension of the PHPMA₁₄₀ precursor with a M_n of 46 300 and M_w/M_n of 1.15 being obtained when targeting PHPMA₁₆₀-PGMA₉₀ (see Fig. S6† and Fig. 3a); synthetic details for related diblock copolymers are summarized in Table S2.† The methanolic co-solvent was then removed from the reaction mixture under reduced pressure and the resulting aqueous solution was freeze-dried to obtain a copolymer powder. Redispersion of this copolymer in ice-cold water at 10% w/w and pH 7, followed by warming to 20 °C led to *in situ* self-assembly of the amphiphilic PHPMA-PGMA diblock copolymer chains to afford either spherical (see Fig. 3b and c) or worm-like nanoparticles (see Fig. 3d), depending on the precise diblock copolymer composition.[82] Furthermore, the resulting worm-like nanoparticles displayed thermoresponsive behavior, as evidenced by temperature-dependent rheology experiments (see Fig. 3e). At room temperature, the worm-like nanoparticles form a percolating 3D network to produce a free-standing gel.[67] However, when cooled, these worm-like nanoparticles undergo a morphological transition to form non-interacting spherical nanoparticles, thus producing a free-flowing liquid. Similar thermoresponsive behavior for PGMA-PHPMA nano-objects prepared by conventional PISA has been widely reported.[43,45,72,80,101] Although the above RAFT solution polymerization protocol was undoubtedly successful, we wished to examine whether wholly aqueous *reverse sequence* PISA formulations were feasible.

Recently, we reported that poly(isopropylideneglycerol monomethacrylate) (PIPGMA) particles prepared *via* RAFT aqueous emulsion polymerization of IPGMA can be readily converted into water-soluble PGMA chains *via* acid hydrolysis.[102] Accordingly, water-miscible GMA was replaced with water-immiscible IPGMA monomer (see Fig. 4a). Thus, a precursor cationic PHPMA₁₄₀ latex (prepared at 10% w/w solids using MPETTC) was chain-extended *via* seeded RAFT aqueous emulsion polymerization of IPGMA using a one-pot protocol, targeting a final diblock composition of PHPMA₁₄₀-PIPGMA₅₅ at 14% w/w solids. Unlike GMA, the water-immiscible IPGMA monomer is preferentially located within the hydrophobic PHPMA latex cores, where it can be polymerized with good RAFT control to afford charge-stabilized PHPMA₁₄₀-PIPGMA₅₅ particles within 2 h. TEM and DLS confirmed the presence of large, spherical latex particles with a modest increase in z-average diameter compared to that of the precursor PHPMA₁₄₀ latex (see Fig. S7†). Subsequent acid hydrolysis of the PIPGMA block using HCl (pH ~ 1.2) at 70 °C afforded a 13.2% w/w aqueous dispersion. ^{1}H NMR spectroscopy and
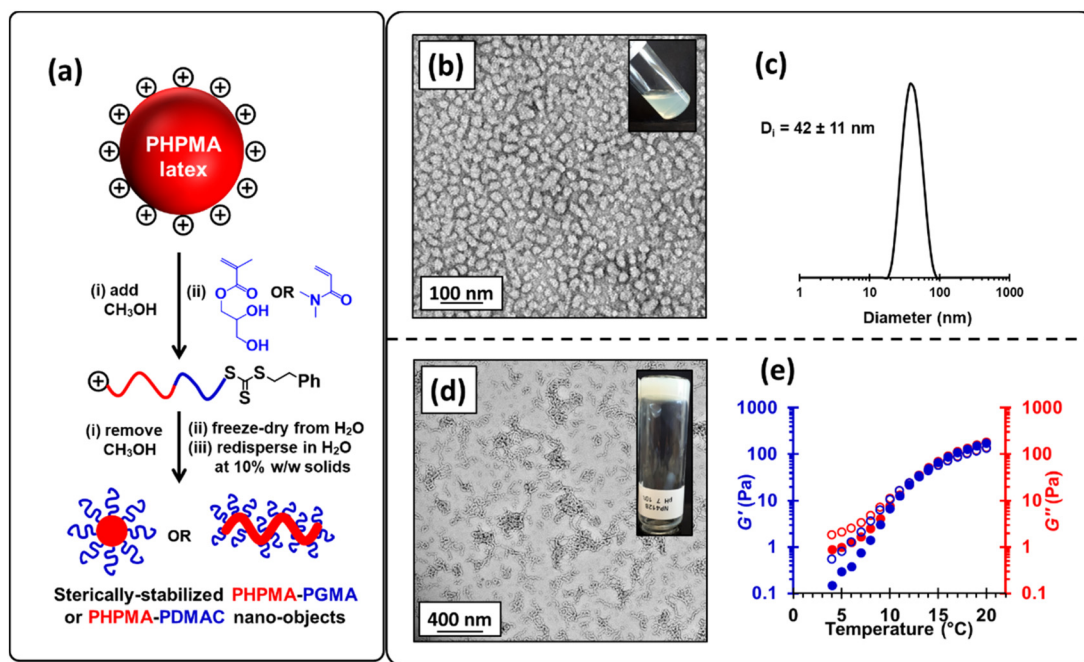
Fig. 3 (a) Schematic representation of a *reverse sequence* PISA synthesis. A charge-stabilized cationic PHPMA latex precursor (prepared by surfactant-free RAFT aqueous dispersion polymerization of HPMA using MPETTC) is first dissolved by adding sufficient methanol co-solvent. The soluble PHPMA chains are then chain-extended *via* RAFT solution polymerization of either GMA or DMAC to produce PHPMA-PGMA or PHPMA-PDMAC diblock copolymers in a water/methanol mixture. Methanol co-solvent is then removed under vacuum prior to freeze-drying from water. Subsequent redispersion of the amphiphilic diblock copolymer chains in initially cold water at 10% w/w solids induces their self-assembly to yield sterically-stabilized nanoparticles. (b) TEM image recorded after drying a 0.1% w/w aqueous dispersion of $PHPMA_{160}$-$PGMA_{90}$ nanoparticles. These nanoparticles formed a free-flowing liquid at 10% w/w solids (see inset digital photograph). (c) DLS particle size distribution data obtained for a 0.1% w/w aqueous dispersion of $PHPMA_{160}$-$PGMA_{90}$ nanoparticles at pH 7 and 20 °C. (d) TEM image recorded after drying a dilute aqueous dispersion of $PHPMA_{160}$-$PGMA_{55}$ nanoparticles at 20 °C. The inset shows a digital photograph of the free-standing 10% w/w worm gel that is formed at 20 °C. (e) Variation in storage (G', filled circles) and loss (G'' open circles) moduli with temperature for a 10% w/w aqueous dispersion of $PHPMA_{160}$-$PGMA_{55}$ nanoparticles at pH 7. The heating sweep (red data) was performed prior to the cooling sweep (blue data). A thermal equilibration time of 5 min was allowed for each 1 °C increment and data were recorded at 1% applied strain and 1 rad s⁻¹.

TEM studies (see Fig. 4) indicate that the charge-stabilized $PHPMA_{140}$-$PIPGMA_{55}$ latex is transformed into sterically-stabilized $PHPMA_{140}$-$PGMA_{55}$ spherical nanoparticles. This is an example of *reverse sequence* PISA because the hydrophobic structure-directing block is synthesized first, rather than last.[68]

Chain extension of a PHPMA latex with DMAC to afford PHPMA-PDMAC nano-objects

So far, we have demonstrated that PHPMA latexes can be chain-extended using a wholly aqueous formulation when employing a *water-immiscible* monomer (*i.e.* IPGMA). An alternative strategy is *molecular dissolution* of the PHPMA latex using a *water-miscible co-solvent*. In principle, this provides an opportunity to prepare new PHPMA-based diblock copolymers, where the water-soluble block is, for example, poly(*N,N′*-dimethylacrylamide) (PDMAC). Notably, well-defined PDMAC-PHPMA diblock copolymers cannot be prepared using a conventional PISA formulation. This is because the hydrophilic PDMAC precursor cannot be efficiently chain-extended using a methacrylic monomer such as HPMA since fragmentation of the radical intermediate preferentially forms the methacrylic tertiary radical rather than the acrylamide-based

secondary radical, thus resulting in a mixture of PDMAC and PHPMA homopolymers.[103–105] This is a well-known limitation of RAFT chemistry: methacrylates must be polymerized before acrylamides for efficient radical cross-over.[106] Similar synthetic problems have been recently reported by Tan and co-workers when attempting to chain-extend a hydrophilic acrylic block with HPMA.[107]

Accordingly, we added sufficient methanol co-solvent to dissolve an aqueous dispersion of cationic $PHPMA_{140}$ latex particles to prepare a range of PHPMA-PDMAC diblock copolymers in the resulting water/methanol binary mixture (see Fig. S8† and Fig. 3a). Representative kinetic data for the RAFT solution polymerization of DMAC using a $PHPMA_{140}$ precursor in a 68 : 32 v/v water/methanol mixture at 56 °C are shown in Fig. S8.† When targeting a PDMAC DP of 160, more than 90% DMAC conversion was achieved within 4 h with good RAFT control, as demonstrated by the linear evolution of M_n with monomer conversion and narrow dispersities. Informed by such kinetic experiments, a precursor $PHPMA_{140}$ latex (M_n = 29 300, M_w/M_n = 1.10) was molecularly dissolved *via* methanol addition and the resulting $PHPMA_{140}$ chains were then chain-extended to prepare a $PHPMA_{140}$-$PDMAC_{160}$ diblock copolymer

Fig. 4 (A) Reaction scheme for the surfactant-free one-pot synthesis of sterically-stabilized PHPMA$_{140}$-PGMA$_{55}$ spherical nanoparticles. A charge-stabilized cationic PHPMA$_{140}$ precursor latex is chain-extended via RAFT emulsion polymerization of IPGMA to afford a charge-stabilized PHPMA$_{140}$-PIPGMA$_{55}$ diblock copolymer latex. Subsequent acid hydrolysis at pH 1.2 affords sterically-stabilized PHPMA$_{140}$-PGMA$_{55}$ spheres. (B) ^{1}H NMR spectra recorded for PHPMA$_{140}$-PIPGMA$_{55}$ and PHPMA$_{140}$-PGMA$_{55}$ diblock copolymers in d$_7$-DMF. Hydrolysis of PHPMA$_{140}$-PIPGMA$_{55}$ to form PHPMA$_{140}$-PGMA$_{55}$ is confirmed by the disappearance of the six methyl protons (black arrows) at 1.36 ppm and 1.44 ppm associated with the acetone protecting group. (C) DMF GPC curves recorded for the PHPMA$_{140}$, PHPMA$_{140}$-PIPGMA$_{55}$ and PHPMA$_{140}$-PGMA$_{55}$. Molecular weight data are expressed relative to a series of near-monodisperse poly(methyl methacrylate) calibration standards. (D) TEM image obtained after drying a 0.1% w/w dispersion of sterically-stabilized PHPMA$_{140}$-PGMA$_{55}$ nanoparticles at pH 1.2.

(M_n = 39 800, M_w/M_n = 1.17). DMF GPC analysis indicated a relatively high blocking efficiency for the PHPMA chains. The methanol co-solvent was then removed under reduced pressure, followed by freeze-drying to afford a PHPMA$_{140}$-PDMAC$_{160}$ diblock copolymer powder. Subsequent redispersion of these amphiphilic copolymer chains in initially ice-cold water (to ensure molecular dissolution of the PHPMA chains)[82] at 10% w/w solids resulted in the formation of spherical nanoparticles (z-average diameter = 41 ± 12 nm; see Fig. 5), with the hydrophilic PDMAC block conferring steric stabilization.[82] Similarly, adjusting the diblock copolymer composition to target PHPMA$_{160}$-PDMAC$_{40}$ (M_n = 34 500, M_w/M_n = 1.13) resulted in the formation of a free-flowing liquid at 5 °C. At its native solution pH of 4.7, this 10% w/w copolymer dispersion underwent a thermoreversible sol–gel transition on heating to form a soft, free-standing gel at 20 °C with a bulk modulus, G', of 97 Pa (see Fig. S9†).[80]

Precursor latex based on an acrylamide-based monomer

We also wished to examine whether other water-miscible monomers could be used to form charge-stabilized precursor latexes. In principle, diacetone acrylamide (DAAM) should be a suitable monomer.[108–113] In order to prepare such PDAAM latexes, an appropriate RAFT agent was selected and the solu-

tion pH was adjusted to ensure colloidal stabilization. Accordingly, a PDAAM$_{99}$ latex was prepared at 10% w/w solids via RAFT aqueous dispersion polymerization of DAAM using a carboxylic acid-functionalized PETTC RAFT agent at pH 7 to confer anionic surface charge and hence charge stabilization. More than 99% DAAM conversion was achieved and GPC analysis indicated an M_n of 22 600 and an M_w/M_n of 1.18 (see Scheme S2†). DLS studies of this precursor PDAAM latex gave a z-average diameter of 71 nm and a polydispersity index of 0.12.

Chain extension was achieved via RAFT solution polymerization of DMAC in a 61 : 39 w/w water/methanol mixture to afford a well-defined PDAAM$_{99}$-PDMAC$_{40}$ diblock copolymer (M_n = 25 400, M_w/M_n = 1.21; see Scheme S2†). This proof-of-concept experiment confirms that this new *reverse sequence* PISA route is applicable to acrylamide-based monomers as well as methacrylic monomers, which significantly broadens the scope of this strategy.

Synthesis of latex precursors *via* RAFT aqueous emulsion polymerization

So far, we have focused on water-miscible monomers for the synthesis of the charge-stabilized precursor latex. However, RAFT PISA of water-immiscible monomers has been widely

Fig. 5 (A) Chemical structure of the PHPMA$_{140}$-PDMAC$_{160}$ diblock copolymer. (B) DMF GPC curves recorded for the PHPMA$_{140}$ precursor and the final PHPMA$_{140}$-PDMAC$_{160}$ diblock copolymer. Molecular weight data are expressed relative to a series of near-monodisperse poly(methyl methacrylate) calibration standards. (C) TEM images recorded after drying a 0.1% w/w dispersion of PHPMA$_{140}$-PDMAC$_{160}$ nanoparticles, indicating a pseudo-spherical morphology. Intensity-average particle size distribution obtained by dynamic light scattering studies of a 0.1% w/w dispersion of cationic PHPMA$_{140}$ latex particles at pH 3.

reported in the PISA literature.[57,58,114–126] Interestingly, many RAFT aqueous emulsion polymerization formulations only yield kinetically-trapped spheres.[78,114,124,127–129] Recently, we reported the synthesis of sterically-stabilized spheres, worms or vesicles *via* RAFT aqueous emulsion polymerization of MOEMA by systematic variation of the target DP of the PMOEMA block while employing a relatively short steric stabilizer block. This was rationalized in terms of the

relatively high aqueous solubility of the MOEMA monomer (19.6 g dm^{-3} at 70 °C) compared to many other water-immiscible vinyl monomers. In view of this prior study, we selected MOEMA for the *reverse sequence* aqueous PISA formulations described herein.

More specifically, MOEMA was polymerized using MPETTC at pH 3 to ensure protonation of this RAFT agent's morpholine group (Fig. 6a). Initial scoping experiments indicated that stable PMOEMA latexes could be consistently obtained between 5.0 and 7.5% w/w solids when conducting the RAFT aqueous emulsion polymerization of MOEMA at 56 °C. Further experiments confirmed that minimal latex coagulation was observed for syntheses conducted at up to 10% w/w solids but extensive coagulation was observed at either 15 or 20% w/w solids (see Fig. S10†). Kinetic data were obtained for the RAFT emulsion polymerization of MOEMA when targeting a PMOEMA DP of 60 and 7.5% w/w solids at 56 °C. In this experiment, aliquots were periodically extracted from the reaction mixture and analysed by ^{1}H NMR spectroscopy and GPC (Fig. 7).

The MOEMA conversion remained relatively low for the first 100 min. This slow initial stage is most likely related to the relatively low concentration of this monomer within the aqueous phase, although induction periods for RAFT polymerizations appear to be a more general phenomenon.[130] Nevertheless, micellar nucleation occurs at around 10% conversion, which corresponds to an instantaneous PMOEMA DP of just 6. Monomer then diffuses from the monomer droplet reservoirs into these nascent particles, leading to a relatively high local concentration and hence the observed rapid rate acceleration (Fig. 7a). A final MOEMA conversion of more than 99% is achieved within the following 140 min, giving a total reaction time of 4 h at 56 °C. The evolution in the molecular weight distribution for this first-stage polymerization was assessed by GPC. The number-average molecular weight (M_n) increased linearly with monomer conversion, indicating that this MOEMA polymerization proceeds with good RAFT control (Fig. 7b). Moreover, dispersities remained low ($M_w/M_n < 1.20$) throughout the polymerization.
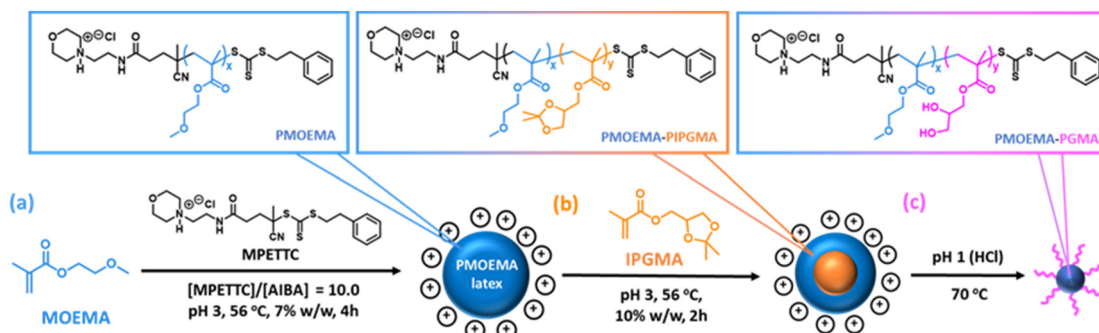
Fig. 6 Schematic representation of a *reverse sequence* aqueous PISA formulation based on the RAFT aqueous emulsion polymerization of 2-methoxyethyl methacrylate (MOEMA). (a) Formation of the cationic PMOEMA latex precursor. (b) Chain extension of the PMOEMA chains with isopropylideneglycerol monomethacrylate (IPGMA) to form a PIPGMA-PMOEMA core–shell latex. (c) Deprotection of the hydrophobic PIPGMA block *via* acid hydrolysis to produce hydrophilic PGMA chains and hence amphiphilic PMOEMA-PGMA diblock copolymer nanoparticles.

Fig. 7 Kinetic data obtained for the RAFT aqueous emulsion polymerization of MOEMA using a cationic MPETTC RAFT agent at 56 °C and the subsequent extension of the PMOEMA chains with IPGMA: (a) monomer conversion *vs.* time curves; (b) evolution in number-average molecular weight (M_n) and dispersity (M_w/M_n) with monomer conversion. Polymerization conditions: [MOEMA]/[MPETTC] molar ratio = 60, [IPGMA]/[PMOEMA$_{60}$] = 27, [MPETTC]/[AIBA] molar ratio = 5.0, targeting 7.5% w/w solids at pH 3. (c) DMF GPC curves recorded for PMOEMA$_{60}$ and PMOEMA$_{60}$-PIPGMA$_{27}$. Molecular weight data are expressed relative to a series of near-monodisperse poly(methyl methacrylate) calibration standards.

A series of PMOEMA$_x$ latexes were prepared targeting various DPs (x = 20, 30, 40, 50, 60 or 70) to examine the effect of this parameter on the final particle size. ^{1}H NMR studies indicated that more than 99% MOEMA conversion could be obtained in each case.

As expected, GPC analysis confirmed the expected progressive increase in PMOEMA M_n when targeting higher x values, with minimal increase in the final M_w/M_n (Fig. 8a). Each PMOEMA latex was then diluted to 0.1% w/w and analyzed by DLS to determine its z-average diameter. A monotonic increase in particle size was observed with increasing DP, with a z-average diameter of more than 200 nm being obtained when targeting PMOEMA$_{70}$ (Fig. 8b).

The initial PMOEMA seed latex was then chain-extended with IPGMA to produce a diblock copolymer latex. Empirically, we found that a one-pot synthesis protocol prevented multimodal molecular weight distributions. Thus, IPGMA is added to the reaction mixture just as the initial MOEMA polymeriz-

Fig. 8 (a) Normalized DMF GPC curves (refractive index detector; calibrated using a series of poly(methyl methacrylate) standards) recorded for six cationic PMOEMA latexes where the PMOEMA DP was systematically varied from 20 to 70. (b) Variation in z-average diameter and DLS polydispersity (PDI) *vs.* PMOEMA M_n for the same series of six PMOEMA latexes.

ation approaches full conversion (with no further AIBA initiator being required). The water-immiscible IPGMA monomer diffuses through the aqueous phase and the second-stage polymerization takes place within the IPGMA-swollen PMOEMA latex particles. IPGMA has a significantly lower aqueous solubility than MOEMA,[102] so PIPGMA is expected to be more hydrophobic than PMOEMA. Hence the PIPGMA block should form the latex core while the PMOEMA block forms the shell, as depicted schematically in Fig. 6.

Kinetic data were also obtained for the IPGMA polymerization. In this case, no induction period was observed and approximately 87% conversion can be achieved within 210 min at 56 °C (see Fig. 7a). GPC analysis confirmed that the M_n for the diblock copolymer chains increased linearly with IPGMA conversion and M_w/M_n values remained below 1.20. Moreover, a relatively high blocking efficiency was observed for the PMOEMA precursor chains. Thus, good RAFT control is also achieved for the second-stage IPGMA polymerization.

The pH-responsive behavior of the PMOEMA-PIPGMA latex particles was assessed by DLS and aqueous electrophoresis (Fig. S11†). Zeta potentials ranging from +10 to +15 mV were observed between pH 2 and pH 5 because the morpholine-based RAFT end-groups are protonated under such conditions and thus confer cationic surface charge. Above pH 5,

these tertiary amine groups gradually became deprotonated, leading to an isoelectric point at around pH 7. DLS studies confirmed that the latex particles retained their colloidal stability between pH 2.0 and pH 5.8. However, the near-neutral latex particles began to flocculate above the latter pH, with macroscopic precipitation being observed at pH 6.5.

Deprotection of PMOEMA-PIPGMA latex to form PMOEMA-PGMA nanoparticles

As reported by Jesson *et al.*, PIPGMA can be readily converted into PGMA *via* acid hydrolysis.[102] Because PGMA is hydrophilic, acid hydrolysis of the hydrophobic PIPGMA block should lead to the *in situ* formation of an amphiphilic PMOEMA-PGMA diblock copolymer. Accordingly, acid hydrolysis of the PIPGMA block was performed at pH 1: ^{1}H NMR spectroscopy studies confirmed that essentially all of the IPGMA repeat units were converted into GMA repeat units within 3 h at 70 °C (Fig. S12†). This drives a dramatic change in copolymer morphology: the double-hydrophobic PMOEMA-PIPGMA chains within the relatively large charge-stabilized latex particles rearrange to form much smaller sterically-stabilized diblock copolymer nanoparticles with PGMA now acting as the steric stabilizer. Indeed, the initial milky-white dispersion becomes a relatively transparent dispersion (see inset digital photographs in Fig. 9). Moreover, DLS studies indicated that the z-average diameter is significantly reduced from 145 nm for the PMOEMA$_{40}$-PIPGMA$_{27}$ precursor latex to just 23 nm for the final PMOEMA$_{40}$-PGMA$_{27}$ nanoparticles (Fig. 9a). TEM images recorded before and after hydrolysis followed by dialysis (Fig. 9b & c) confirmed that the precursor latex particles are converted into much finer spherical nanoparticles after hydrolysis. Furthermore, there is minimal difference between the GPC traces recorded for the initial PMOEMA$_{40}$-PIPGMA$_{27}$ PMOEMA$_{40}$-PGMA$_{27}$ and final PMOEMA$_{40}$-PGMA$_{27}$ diblock copolymer chains (Fig. S13†). The resulting aqueous dispersion of PMOEMA-PGMA nanoparticles was subsequently dialyzed against deionized water overnight to remove small molecule impurities (excess acid, traces of acetone, spent initiator *etc.*).

After dialysis, the final pH of the aqueous dispersion was essentially that of deionized water (pH ~ 6). In summary, a rather efficient *reverse sequence* PISA formulation has been developed based on RAFT aqueous emulsion polymerization.

DLS and aqueous electrophoresis were used to assess the pH-responsive behavior of the nanoparticles obtained after deprotection of the PIPGMA block (Fig. S11c†). At pH 2, the sterically-stabilized PMOEMA$_{40}$-PGMA$_{27}$ nanoparticles exhibited a zeta potential of +10 mV owing to the protonated morpholine-based RAFT end-groups. An isoelectric point was observed at pH 5 and the zeta potential became −10 mV at pH 8.

This weakly anionic character is attributed to the presence of a small number of methacrylic acid (MAA) repeat units within the PGMA stabilizer block owing to partial hydrolysis of methacrylic ester bonds. Thus, acetone deprotection of the IPGMA residues *via* acid hydrolysis is not perfectly selective. Further investigations indicated that approximately one MAA unit was produced per diblock copolymer chain. It was hypothesized that performing the hydrolysis at pH 2 might prevent ester hydrolysis. Unfortunately, these milder conditions required much longer reaction times to achieve complete deprotection but did not prevent this unwanted side-reaction. Unlike the precursor PMOEMA$_{40}$-PIPGMA$_{27}$ latex particles, the PMOEMA$_{40}$-PGMA$_{27}$ nanoparticles remained colloidally stable across the entire pH range studied owing to the steric stabilization conferred by the hydrophilic PGMA block.

Effect of added salt on the copolymer morphology

Varying amounts of NaCl were added to a 7.3% w/w aqueous dispersion of PMOEMA$_{40}$-PGMA$_{27}$ spherical nanoparticles to produce salt concentrations of 50, 100 or 150 mM, respectively. In the presence of 50 mM NaCl, the dispersion became significantly more turbid and viscous but remained a free-flowing fluid. In contrast, a free-standing gel was obtained in the presence of either 100 or 150 mM NaCl (Fig. 10). According to the PISA literature, this suggests a salt-induced sphere-to-worm morphology transition.[131]

TEM studies confirmed that a sphere-to-worm transition occurred in the presence of sufficient NaCl (Fig. 10). The
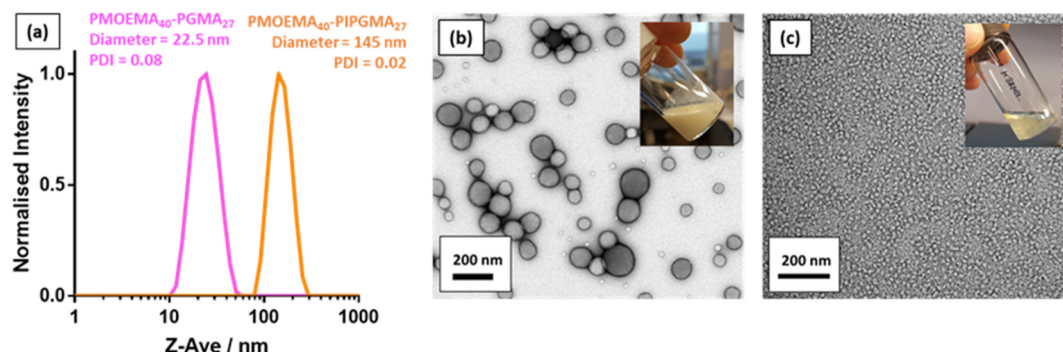
Fig. 9 (a) Normalized DLS intensity-average particle size distributions recorded at 20 °C for 0.1% w/w aqueous dispersions of (i) charge-stabilized PMOEMA$_{40}$-PIPGMA$_{27}$ latex particles and (ii) sterically-stabilized PMOEMA$_{40}$-PGMA$_{27}$ nanoparticles. (b) TEM image recorded after drying the PMOEMA$_{40}$-PIPGMA$_{27}$ latex, which formed a free-flowing turbid dispersion at 8.2% w/w solids (see inset digital photograph). (c) TEM image recorded after drying an aqueous dispersion of PMOEMA$_{40}$-PGMA$_{27}$ nanoparticles (after dialysis against deionized water). These nanoparticles afford a relatively transparent free-flowing dispersion at 7.3% w/w solids (see inset digital photograph).

Fig. 10 Digital photograph (left) illustrating the effect of addition of 50–150 mM NaCl to an aqueous dispersion of PMOEMA$_{40}$-PGMA$_{27}$ nano-particles at pH 6 to produce a soft free-standing gel at 20 °C. The corresponding TEM image (right) confirms the anisotropic worm-like particles that are formed in the presence of 150 mM NaCl. The inset image shows a shear-induced polarized light image of the corresponding 7.3% w/w worm dispersion recorded at a maximum shear rate of 1.0 s^{-1}. The Maltese cross motif indicates birefringence arising from the *in situ* worm alignment that occurs under such conditions.[132]

added salt screens the anionic charge arising from the MAA repeat unit(s) within the otherwise neutral PGMA chains, which enables the amphiphilic PMOEMA$_{40}$-PGMA$_{27}$ chains to self-assemble to form worms. In contrast, mutual repulsion between the weakly anionic spheres formed in the absence of any added salt prevents their stochastic 1D fusion to form worms.[39] It is well-known that highly anisotropic worms can form a 3D percolating network *via* multiple inter-worm contacts, which enables the formation of a free-standing gel at relatively low copolymer concentration.[67] Moreover, shear-induced polarized light imaging (SIPLI) studies[133] of the free-standing gel recorded at 20 °C under constant shear produced a distinctive Maltese cross motif (see inset within TEM image shown in Fig. 10), which is characteristic of the shear-induced alignment of anisotropic worms.[45]

Conclusions

We report new surfactant-free aqueous PISA formulations that enable the structure-directing hydrophobic block to be synthesized first when targeting amphiphilic diblock copolymers. This counter-intuitive *reverse sequence* approach requires an ionic RAFT agent to confer charge stabilization on the precursor latex, which can be prepared *via* RAFT aqueous *dispersion* polymerization of 2-hydroxypropyl methacrylate (HPMA). Unfortunately, attempted chain extension of this PHPMA latex precursor using *water-miscible* monomers only led to their uncontrolled free radical polymerization in the aqueous phase. However, chain extension utilizing a *water-immiscible* monomer, isopropylideneglycerol monomethacrylate (IPGMA), afforded a charge-stabilized PHPMA-PIPGMA diblock copolymer latex; this is because the water-immiscible IPGMA monomer preferentially partitions into the latex core. Subsequent acid hydrolysis afforded the desired sterically-stabilized PHPMA-PGMA nano-objects. Alternatively, addition

of methanol to solubilize the precursor PHPMA latex enables efficient chain extension *via* RAFT *solution* polymerization in water/methanol binary mixtures. This protocol enables the formation of both PHPMA-PGMA diblock copolymer nanoparticles and also new copolymer examples that cannot be accessed *via* conventional aqueous PISA. Moreover, this counter-intuitive *reverse sequence* PISA approach is also applicable to acrylamide-based monomers. Finally, charge-stabilized poly(2-methoxyethyl methacrylate) (PMOEMA) latexes were prepared *via* RAFT aqueous *emulsion* polymerization. Subsequent chain extension using IPGMA leads to a charge-stabilized PMOEMA-PIPGMA diblock copolymer latex of approximately 150 nm diameter. Finally, acid-catalyzed removal of the acetone protecting groups from the PIPGMA block affords amphiphilic PMOEMA-PGMA diblock copolymer chains that undergo *in situ* self-assembly to form sterically-stabilized diblock copolymer nanoparticles. Given the excellent control over molecular weight distribution, relatively high atom economy and minimal levels of residual monomer, we envisage that such new *reverse sequence* PISA routes are likely to become a useful addition to the synthetic polymer chemist's toolbox for the rational synthesis of functional block copolymer nanoparticles.

Conflicts of interest

There are no conflicts to declare.

Acknowledgements

References

1 S. L. Canning, G. N. Smith and S. P. Armes, *Macromolecules*, 2016, **49**, 1985–2001.

2 N. J. W. Penfold, J. Yeow, C. Boyer and S. P. Armes, *ACS Macro Lett.*, 2019, **8**, 1029–1054.

3 H. Phan, V. Taresco, J. Penelle and B. Couturaud, *Biomater. Sci.*, 2021, **9**, 38–50.

4 N. J. Warren and S. P. Armes, *J. Am. Chem. Soc.*, 2014, **136**, 10174–10185.

5 F. D'Agosto, J. Rieger and M. Lansalot, *Angew. Chem., Int. Ed.*, 2020, **59**, 8368–8392.

6 B. Charleux, G. Delaittre, J. Rieger and F. D'Agosto, *Macromolecules*, 2012, **45**, 6753–6765.

7 A. B. Lowe, *Polymer*, 2016, **106**, 161–181.

8 M. J. Derry, L. A. Fielding and S. P. Armes, *Prog. Polym. Sci.*, 2016, **52**, 1–18.

9 C. Liu, C. Y. Hong and C. Y. Pan, *Polym. Chem.*, 2020, **11**, 3673–3689.

10 J. Yeow and C. Boyer, *Adv. Sci.*, 2017, **4**, 1700137.

11 W. J. Zhang, C. Y. Hong and C. Y. Pan, *Macromol. Rapid Commun.*, 2019, **40**, e1800279.

12 M. J. Derry, L. A. Fielding, N. J. Warren, C. J. Mable, A. J. Smith, O. O. Mykhaylyk and S. P. Armes, *Chem. Sci.*, 2016, **7**, 5078–5090.

13 R. Takahashi, S. Miwa, F. H. Sobotta, J. H. Lee, S. Fujii, N. Ohta, J. C. Brendel and K. Sakurai, *Polym. Chem.*, 2020, **11**, 1514–1524.

14 A. Czajka and S. P. Armes, *Chem. Sci.*, 2020, **11**, 11443–11454.

15 E. E. Brotherton, F. L. Hatton, A. A. Cockram, M. J. Derry, A. Czajka, E. J. Cornel, P. D. Topham, O. O. Mykhaylyk and S. P. Armes, *J. Am. Chem. Soc.*, 2019, **141**, 13664–13675.

16 J. Chiefari, J. Jeffery, R. T. A. Mayadunne, G. Moad, E. Rizzardo and S. H. Thang, *Macromolecules*, 1999, **32**, 7700–7702.

17 R. T. A. Mayadunne, E. Rizzardo, J. Chiefari, Y. K. Chong, G. Moad and S. H. Thang, *Macromolecules*, 1999, **32**, 6977–6980.

18 G. Moad, Y. K. Chong, A. Postma, E. Rizzardo and S. H. Thang, *Polymer*, 2005, **46**, 8458–8468.

19 S. Perrier, *Macromolecules*, 2017, **50**, 7433–7447.

20 D. J. Keddie, G. Moad, E. Rizzardo and S. H. Thang, *Macromolecules*, 2012, **45**, 5321–5342.

21 B. R. Parker, M. J. Derry, Y. Ning and S. P. Armes, *Langmuir*, 2020, **36**, 3730–3736.

22 D. Zehm, L. P. D. Ratcliffe and S. P. Armes, *Macromolecules*, 2013, **46**, 128–139.

23 M. J. Derry, T. Smith, P. S. O'Hora and S. P. Armes, *ACS Appl. Mater. Interfaces*, 2019, **11**, 33364–33369.

24 C. György, S. J. Hunter, C. Girou, M. J. Derry and S. P. Armes, *Polym. Chem.*, 2020, **11**, 4579–4590.

25 E. R. Jones, M. Semsarilar, P. Wyman, M. Boerakker and S. P. Armes, *Polym. Chem.*, 2016, **7**, 851–859.

26 M. Semsarilar, N. J. W. Penfold, E. R. Jones and S. P. Armes, *Polym. Chem.*, 2015, **6**, 1751–1757.

27 M. Semsarilar, V. Ladmiral, A. Blanazs and S. P. Armes, *Polym. Chem.*, 2014, **5**, 3466–3475.

28 L. A. Fielding, M. J. Derry, V. Ladmiral, J. Rosselgong, A. M. Rodrigues, L. P. D. Ratcliffe, S. Sugihara and S. P. Armes, *Chem. Sci.*, 2013, **4**, 2081–2087.

29 L. P. D. Ratcliffe, M. J. Derry, A. Ianiro, R. Tuinier and S. P. Armes, *Angew. Chem.*, 2019, **131**, 19140–19146.

30 M. J. Rymaruk, S. J. Hunter, C. T. O'Brien, S. L. Brown, C. N. Williams and S. P. Armes, *Macromolecules*, 2019, **52**, 2822–2832.

31 Q. Zhang and S. Zhu, *ACS Macro Lett.*, 2015, **4**, 755–758.

32 V. J. Cunningham, M. J. Derry, L. A. Fielding, O. M. Musa and S. P. Armes, *Macromolecules*, 2016, **49**, 4520–4533.

33 Y. Ning, L. Han, M. J. Derry, F. C. Meldrum and S. P. Armes, *J. Am. Chem. Soc.*, 2019, **141**, 2557–2567.

34 C. J. Mable, N. J. Warren, K. L. Thompson, O. O. Mykhaylyk and S. P. Armes, *Chem. Sci.*, 2015, **6**, 6179–6188.

35 K. L. Thompson, C. J. Mable, A. Cockram, N. J. Warren, V. J. Cunningham, E. R. Jones, R. Verber and S. P. Armes, *Soft Matter*, 2014, **10**, 8615–8626.

36 C. A. Figg, A. Simula, K. A. Gebre, B. S. Tucker, D. M. Haddleton and B. S. Sumerlin, *Chem. Sci.*, 2015, **6**, 1230–1236.

37 G. Mellot, J. M. Guigner, L. Bouteiller, F. Stoffelbach and J. Rieger, *Angew. Chem., Int. Ed.*, 2019, **58**, 3173–3177.

38 D. E. Mitchell, J. R. Lovett, S. P. Armes and M. I. Gibson, *Angew. Chem., Int. Ed.*, 2016, **55**, 2801–2804.

39 J. R. Lovett, N. J. Warren, L. P. D. Ratcliffe, M. K. Kocik and S. P. Armes, *Angew. Chem., Int. Ed.*, 2015, **54**, 1279–1283.

40 X. Wang, S. Man, J. Zheng and Z. An, *ACS Macro Lett.*, 2018, **7**, 1461–1467.

41 L. D. Blackman, S. Varlas, M. C. Arno, A. Fayter, M. I. Gibson and R. K. O'Reilly, *ACS Macro Lett.*, 2017, **6**, 1263–1267.

42 L. D. Blackman, S. Varlas, M. C. Arno, Z. H. Houston, N. L. Fletcher, K. J. Thurecht, M. Hasan, M. I. Gibson and R. K. O'Reilly, *ACS Cent. Sci.*, 2018, **4**, 718–723.

43 I. Canton, N. J. Warren, A. Chahal, K. Amps, A. Wood, R. Weightman, E. Wang, H. Moore and S. P. Armes, *ACS Cent. Sci.*, 2016, **2**, 65–74.

44 R. Deng, M. J. Derry, C. J. Mable, Y. Ning and S. P. Armes, *J. Am. Chem. Soc.*, 2017, **139**, 7616–7623.

45 N. J. Warren, M. J. Derry, O. O. Mykhaylyk, J. R. Lovett, L. P. D. Ratcliffe, V. Ladmiral, A. Blanazs, L. A. Fielding and S. P. Armes, *Macromolecules*, 2018, **51**, 8357–8371.

46 X. Wang, J. Zhou, X. Lv, B. Zhang and Z. An, *Macromolecules*, 2017, **50**, 7222–7232.

47 C. J. Mable, M. J. Derry, K. L. Thompson, L. A. Fielding, O. O. Mykhaylyk and S. P. Armes, *Macromolecules*, 2017, **50**, 4465–4473.

48 C. A. Figg, R. N. Carmean, K. C. Bentz, S. Mukherjee, D. A. Savin and B. S. Sumerlin, *Macromolecules*, 2017, **50**, 935–943.

49 S. J. Byard, M. Williams, B. E. McKenzie, A. Blanazs and S. P. Armes, *Macromolecules*, 2017, **50**, 1482–1493.

50 J. R. Lovett, N. J. Warren, S. P. Armes, M. J. Smallridge and R. B. Cracknell, *Macromolecules*, 2016, **49**, 1016–1025.

51 N. J. Warren, J. Rosselgong, J. Madsen and S. P. Armes, *Biomacromolecules*, 2015, **16**, 2514–2521.

52 S. Sugihara, A. H. Ma'Radzi, S. Ida, S. Irie, T. Kikukawa and Y. Maeda, *Polymer*, 2015, **76**, 17–24.

53 P. Galanopoulo, P. Y. Dugas, M. Lansalot and F. D'Agosto, *Polym. Chem.*, 2020, **11**, 3922–3930.

54 M. Chenal, J. Rieger, C. Vechambre, J.-M. Chenal, L. Chazeau, C. Creton and L. Bouteiller, *Macromol. Rapid Commun.*, 2013, 1524–1529.

55 C. J. Mable, R. R. Gibson, S. Prevost, B. E. McKenzie, O. O. Mykhaylyk and S. P. Armes, *J. Am. Chem. Soc.*, 2015, **137**, 16098–16108.

56 W. Zhang, F. D'Agosto, P. Y. Dugas, J. Rieger and B. Charleux, *Polymer*, 2013, **54**, 2011–2019.

57 A. A. Cockram, T. J. Neal, M. J. Derry, O. O. Mykhaylyk, N. S. J. Williams, M. W. Murray, S. N. Emmett and S. P. Armes, *Macromolecules*, 2017, **50**, 796–802.

58 F. L. Hatton, J. R. Lovett and S. P. Armes, *Polym. Chem.*, 2017, **8**, 4856–4868.

59 T. R. Guimarães, Y. L. Bong, S. W. Thompson, G. Moad, S. Perrier and P. B. Zetterlund, *Polym. Chem.*, 2021, **12**, 122–133.

60 C. György, J. R. Lovett, N. J. W. Penfold and S. P. Armes, *Macromol. Rapid Commun.*, 2019, **40**, 1–7.

61 S. Y. Khor, N. P. Truong, J. F. Quinn, M. R. Whittaker and T. P. Davis, *ACS Macro Lett.*, 2017, **6**, 1013–1019.

62 N. J. Warren, O. O. Mykhaylyk, A. J. Ryan, M. Williams, T. Doussineau, P. Dugourd, R. Antoine, G. Portale and S. P. Armes, *J. Am. Chem. Soc.*, 2015, **137**, 1929–1937.

63 D. L. Beattie, O. O. Mykhaylyk and S. P. Armes, *Chem. Sci.*, 2020, **11**, 10821–10834.

64 M. Sponchioni, C. T. O'Brien, C. Borchers, E. Wang, M. N. Rivolta, N. J. W. Penfold, I. Canton and S. P. Armes, *Chem. Sci.*, 2020, **11**, 232–240.

65 S. J. Byard, C. T. O'Brien, M. J. Derry, M. Williams, O. O. Mykhaylyk, A. Blanazs and S. P. Armes, *Chem. Sci.*, 2020, **11**, 396–402.

66 C. J. Mable, I. Canton, O. O. Mykhaylyk, B. Ustbas Gul, P. Chambon, E. Themistou and S. P. Armes, *Chem. Sci.*, 2019, **10**, 4811–4821.

67 J. R. Lovett, M. J. Derry, P. Yang, F. L. Hatton, N. J. Warren, P. W. Fowler and S. P. Armes, *Chem. Sci.*, 2018, **9**, 7138–7144.

68 T. J. Neal, N. J. W. Penfold and S. P. Armes, *Angew. Chem., Int. Ed.*, 2022, **61**, e202207376.

69 N. J. W. Penfold, J. R. Lovett, P. Verstraete, J. Smets and S. P. Armes, *Polym. Chem.*, 2017, **8**, 272–282.

70 S. Sugihara, A. Blanazs, S. P. Armes, A. J. Ryan and A. L. Lewis, *J. Am. Chem. Soc.*, 2011, **133**, 15707–15713.

71 A. Blanazs, J. Madsen, G. Battaglia, A. J. Ryan and S. P. Armes, *J. Am. Chem. Soc.*, 2011, **133**, 16581–16587.

72 N. J. Warren, O. O. Mykhaylyk, D. Mahmood, A. J. Ryan and S. P. Armes, *J. Am. Chem. Soc.*, 2014, **136**, 1023–1033.

73 J. Chiefari, Y. K. Chong, F. Ercole, J. Krstina, J. Jeffery, T. P. T. Le, R. T. A. Mayadunne, G. F. Meijs, C. L. Moad, G. Moad, E. Rizzardo and S. H. Thang, *Macromolecules*, 1998, **31**, 5559–5562.

74 G. Moad, E. Rizzardo and S. H. Thang, *Aust. J. Chem.*, 2009, **62**, 1402–1472.

75 G. Moad, E. Rizzardo and S. H. Thang, *Aust. J. Chem.*, 2012, **65**, 985–1076.

76 S. Perrier, *Macromolecules*, 2017, **50**, 7433–7447.

77 G. Moad, E. Rizzardo and S. H. Thang, *Aust. J. Chem.*, 2005, **58**, 379–410.

78 V. J. Cunningham, A. M. Alswieleh, K. L. Thompson, M. Williams, G. J. Leggett, S. P. Armes and O. M. Musa, *Macromolecules*, 2014, **47**, 5613–5623.

79 S. Boisse, J. Rieger, G. Pembouong, P. Beaunier and B. Charleux, *J. Polym. Sci., Part A: Polym. Chem.*, 2011, **49**, 3346–3354.

80 A. Blanazs, R. Verber, O. O. Mykhaylyk, A. J. Ryan, J. Z. Heath, C. W. Douglas and S. P. Armes, *J. Am. Chem. Soc.*, 2012, **134**, 9741–9748.

81 J. Madsen, S. P. Armes, K. Bertal, S. MacNeil and A. L. Lewis, *Biomacromolecules*, 2009, **10**, 1875–1887.

82 M. K. Kocik, O. O. Mykhaylyk and S. P. Armes, *Soft Matter*, 2014, **10**, 3984–3992.

83 N. J. W. Penfold, J. R. Lovett, N. J. Warren, P. Verstraete, J. Smets and S. P. Armes, *Polym. Chem.*, 2016, **7**, 79–88.

84 J. Z. Du, H. Willcock, J. P. Patterson, I. Portman and R. K. O'Reilly, *Small*, 2011, **7**, 2070–2080.

85 R. R. Gibson, S. P. Armes, O. M. Musa and A. Fernyhough, *Polym. Chem.*, 2019, **10**, 1312–1323.

86 D. L. Beattie, O. O. Mykhaylyk, A. J. Ryan and S. P. Armes, *Macromolecules*, 2021, **17**, 5602–5612.

87 D. L. Beattie, O. O. Mykhaylyk, A. J. Ryan and S. P. Armes, *Macromolecules*, 2012, **45**, 5099–5107.

88 A. Lubnin, K. O'Malley, D. Hanshumaker and J. Lai, *Eur. Polym. J.*, 2010, **46**, 1563–1575.

89 J. T. Lai, D. Filla and R. Shea, *Macromolecules*, 2002, **35**, 6754–6756.

90 M. Semsarilar, V. Ladmiral, A. Blanazs and S. P. Armes, *Langmuir*, 2012, **28**, 914–922.

91 M. Semsarilar, E. R. Jones, A. Blanazs and S. P. Armes, *Adv. Mater.*, 2012, **24**, 3378–3382.

92 J. Yeow and C. Boyer, *Adv. Sci.*, 2017, **4**, 1700137.

93 J. Yeow, O. R. Sugita and C. Boyer, *ACS Macro Lett.*, 2016, **5**, 558–564.

94 Y. J. Ma, P. Gao, Y. Ding, L. L. Huang, L. Wang, X. H. Lu and Y. L. Cai, *Macromolecules*, 2019, **52**, 1033–1041.

95 P. Gao, H. Cao, Y. Ding, M. Cai, Z. Cui, X. Lu and Y. Cai, *ACS Macro Lett.*, 2016, **5**, 1327–1331.

96 K. Ferji, P. Venturini, F. Cleymand, C. Chassenieux and J.-L. Six, *Polym. Chem.*, 2018, **9**, 2868–2872.

97 M. Chen, M. Zhong and J. A. Johnson, *Chem. Rev.*, 2016, **116**, 10167–10211.

98 H. Wang, Q. Li, J. Dai, F. Du, H. Zheng and R. Bai, *Macromolecules*, 2013, **46**, 2576–2582.

99 K. Jung, C. Boyer and P. B. Zetterlund, *Polym. Chem.*, 2017, **8**, 3965–3970.

100 W. Smulders, R. G. Gilbert and M. J. Monteiro, *Macromolecules*, 2003, **36**, 4309–4318.

101 K. A. Simon, N. J. Warren, B. Mosadegh, M. R. Mohammady, G. M. Whitesides and S. P. Armes, *Biomacromolecules*, 2015, **16**, 3952–3958.

102 C. P. Jesson, V. J. Cunningham, M. J. Smallridge and S. P. Armes, *Macromolecules*, 2018, **51**, 3221–3232.

103 D. J. Keddie, G. Moad, E. Rizzardo and S. H. Thang, *Macromolecules*, 2012, **45**, 5321–5342.

104 J. Chiefari, R. T. A. Mayadunne, C. L. Moad, G. Moad, E. Rizzardo, A. Postma and S. H. Thang, *Macromolecules*, 2003, **36**, 2273–2283.

105 G. Moad, E. Rizzardo and S. H. Thang, *Aust. J. Chem.*, 2006, **59**, 669–692.

106 C. P. Easterling, Y. Xia, J. Zhao, G. E. Fanucci and B. S. Sumerlin, *ACS Macro Lett.*, 2019, **8**, 1461–1466.

107 Y. X. Zhang, L. L. Yu, X. C. Dai, L. Zhang and J. B. Tan, *ACS Macro Lett.*, 2019, **8**, 1102–1109.

108 J. L. de la Haye, I. Martin-Fabiani, M. Schulz, J. L. Keddie, F. D'Agosto and M. Lansalot, *Macromolecules*, 2017, **50**, 9315–9328.

109 S. Parkinson, N. S. Hondow, J. S. Conteh, R. A. Bourne and N. J. Warren, *React. Chem. Eng.*, 2019, **4**, 852–861.

110 G. Mellot, P. Beaunier, J. M. Guigner, L. Bouteiller, J. Rieger and F. Stoffelbach, *Macromol. Rapid Commun.*, 2019, **40**, e1800315.

111 J. He, Q. Xu, J. Tan, L. Zhang, J. Tan and L. Zhang, *Macromol. Rapid Commun.*, 2019, **40**, e1800296.

112 X. Wang, J. M. Zhou, X. Q. Lv, B. H. Zhang and Z. S. An, *Macromolecules*, 2017, **50**, 7222–7232.

113 X. Wang, C. A. Figg, X. Q. Lv, Y. Q. Yang, B. S. Sumerlin and Z. S. An, *ACS Macro Lett.*, 2017, **6**, 337–342.

114 N. P. Truong, M. V. Dussert, M. R. Whittaker, J. F. Quinn and T. P. Davis, *Polym. Chem.*, 2015, **6**, 3865–3874.

115 S. Boissie, J. Rieger, K. Belal, A. Di-Cicco, P. Beanier, M. H. Li and B. Charleux, *Chem. Commun.*, 2010, **46**, 1950–1952.

116 S. J. Hunter, N. J. W. Penfold, E. R. Jones, T. Zinn, O. O. Mykhaylyk and S. P. Armes, *Macromolecules*, 2022, **55**, 3051–3062.

117 S. J. Hunter, J. R. Lovett, O. O. Mykhaylyk, E. R. Jones and S. P. Armes, *Polym. Chem.*, 2021, **12**, 3629–3639.

118 B. Akpinar, L. A. Fielding, V. J. Cunningham, Y. Ning, O. O. Mykhaylyk, P. W. Fowler and S. P. Armes, *Macromolecules*, 2016, **49**, 5160–5171.

119 C. J. Ferguson, R. J. Hughes, D. Nguyen, B. T. T. Pham, R. G. Gilbert, A. K. Serelis, C. H. Such and B. S. Hawkett, *Macromolecules*, 2005, **38**, 2191–2204.

120 C. J. Ferguson, R. J. Hughes, B. T. T. Pham, B. S. Hawkett, R. G. Gilbert, A. K. Serelis and C. H. Such, *Macromolecules*, 2002, **35**, 9243–9245.

121 F. Stoffelbach, L. Tibiletti, J. Rieger and B. Charleux, *Macromolecules*, 2008, **41**, 7850–7856.

122 J. Rieger, G. Osterwinter, C. Bui, F. Stoffelbnach and B. Charleux, *Macromolecules*, 2009, **42**, 5518–5525.

123 D. Alaimo, C. Jérôme, B. Charleux, F. Stoffelbach, C. Bui and J. Rieger, *Macromolecules*, 2008, **41**, 4065–4068.

124 W. Zhang, F. D'Agosto, O. Boyron, J. Rieger and B. Charleux, *Macromolecules*, 2011, **44**, 7584–7593.

125 M. Khan, T. R. Guimarães, R. P. Kuchel, G. Moad, S. Perrier and P. B. Zetterlund, *Angew. Chem., Int. Ed.*, 2021, **60**, 23281–23288.

126 T. R. Guimarães, M. Khan, R. P. Kuchel, I. C. Morrow, H. Minami, G. Moad, S. Perrier and P. B. Zetterlund, *Macromolecules*, 2019, **52**, 2965–2974.

127 J. Rieger, W. Zhang, F. Stoffelbach and B. Charleux, *Macromolecules*, 2010, **43**, 6302–6310.

128 I. Chaduc, A. Crepet, O. Boyron, B. Charleux, F. D'Agosto and M. Lansalot, *Macromolecules*, 2013, **46**, 6013–6023.

129 I. Chaduc, M. Girod, R. Antoine, B. Charleux, F. D'Agosto and M. Lansalot, *Macromolecules*, 2012, **45**, 5881–5893.

130 K. G. E. Bradford, L. M. Petit, R. Whitfield, A. Anastasaki, C. Barner-Kowollik and D. Konkolewicz, *J. Am. Chem. Soc.*, 2021, **143**, 17769–17777.

131 S. M. North and S. P. Armes, *Polym. Chem.*, 2020, **11**, 2147–2156.

132 O. O. Mykhaylyk, N. J. Warren, A. J. Parnell, G. Pfeifer and J. Laeuger, *J. Polym. Sci., Part B: Polym. Phys.*, 2016, **54**, 2151–2170.

133 A. Blanazs, R. Verber, O. O. Mykhaylyk, A. J. Ryan, J. Z. Heath, C. W. I. Douglas and S. P. Armes, *J. Am. Chem. Soc.*, 2012, **134**, 9741–9748.